Unified description of ultrafast stimulated Raman scattering in optical fibers

Clifford Headley III and Govind P. Agrawal

The Institute of Optics, University of Rochester, Rochester, New York 14627

Received October 2, 1995; revised manuscript received May 22, 1996

Coupled nonlinear equations that describe the nonlinear process of stimulated Raman scattering in optical fibers are derived. These equations account in a unified manner for the Raman amplification, the Stokes generation, the induced self-frequency shift, and the interpulse stimulated Raman-scattering-induced cross-frequency shift. The equations reduce to a well-known form for relatively wide picosecond pump pulses. Using these equations, we show theoretically that the effects of cross-phase modulation, self-frequency shift, and cross-frequency shift cause two optical pulses copropagating in the anomalous dispersion regime of the fiber to shed some of their energy and evolve into a narrower soliton, which has a higher frequency shift than a single propagating soliton. It is also shown that the self-frequency shift of femtosecond pulses is detrimental to Raman generation. As the input pulse width is reduced, the spectrum of the pulse shifts by an amount comparable with the Raman shift. The shift increases continuously with propagation at such a rapid rate that the Stokes pulse has no time to build up from noise to significant energy levels.

1. INTRODUCTION

Raman scattering is a process by which a fraction of the light incident upon a transparent material is shifted downward in frequency through molecular vibrations.[1] For ultrafast pump pulses propagating in an optical fiber this phenomenon can appear in several different forms. The most common manifestation of stimulated Raman scattering (SRS) is Raman generation,[2–4] which describes the Stokes-pulse growth from spontaneously scattered Raman-shifted radiation in the fiber. Raman amplification, the second manifestation, occurs when the energy from an intense pump pulse is transferred to a weaker signal pulse (copropagating or counterpropagating) through SRS.[5] Finally, intrapulse SRS appears as a transfer of energy from high-frequency components of a pulse to the lower-frequency components of the same pulse in a nonlinear phenomenon called the self-frequency shift (SFS).[6–8] These manifestations of SRS have generally been treated as separate problems. The description of Raman generation has used two coupled nonlinear Schrödinger equations, with one equation describing a seed pulse that represents the average properties of the spontaneous Raman noise in the fiber.[2,3] The same set of equations is used to describe Raman amplification, but instead of a seed pulse one of the equations governs the evolution of the weak input signal.[5] Finally, intrapulse SRS is described by a single equation governing the pump pulse evolution, with other manifestations of SRS ignored.[6,7]

Our objective in this paper is to provide a unified framework for SRS phenomenon that occurs when ultrafast pump pulses propagate in a single-mode fiber. To this end, a set of two coupled nonlinear wave equations is derived to describe the various manifestations of SRS in a unified manner. These equations are valid as long as the slowly varying envelope approximation holds and can be applied for pulse widths as short as ~10 fs. For femtosecond copropagating pulses there is a new interpulse SRS effect, referred to here as the cross-frequency shift (CFS),[8] which is a spectral downshift of a pulse because of the presence of a second copropagating pulse. The effect of the CFS and the SFS on Raman generation is also examined.

This paper is organized as follows. In Section 2 an outline of the derivation of the coupled nonlinear Schrödinger equations is given. For picosecond pulses the simplified form of these equations given in Section 3 can be used. The full equations are used in Section 4 to describe the propagation of copropagating ultrashort solitons, and it is shown that the SFS can inhibit the buildup of Stokes light from noise. The results are summarized in Section 5.

2. COUPLED NONLINEAR SCHRÖDINGER EQUATIONS

In previous studies it was pointed out that the polarizability of a molecule is affected on two different time scales during pulse propagation in an optical fiber.[4,9] The first is an essentially instantaneous time scale associated with the electronic response and leads to an intensity-dependent refractive index (Kerr nonlinearity). The second time scale is associated with molecular vibrations and cannot be considered instantaneous because molecules respond over a period of 50–100 fs.[9] In addition, vibrations of the molecule can occur spontaneously through, for example, thermal noise. The total induced polarization, $\mathbf{P}(\mathbf{r}, t)$, which accounts for the linear polarization $\mathbf{P}_L(\mathbf{r}, t)$, the noise-induced polarization $\mathbf{P}_N(\mathbf{r}, t)$, and the third-order nonlinear polarizations that are due to the Kerr effect $\mathbf{P}_K(\mathbf{r}, t)$ and to the Raman effect $\mathbf{P}_R(\mathbf{r}, t)$, can be written as[1,4]

0740-3224/96/1002170-08$10.00

$$\mathbf{P}(\mathbf{r}, t) = \mathbf{P}_L(\mathbf{r}, t) + \mathbf{P}_N(\mathbf{r}, t) + \mathbf{P}_K(\mathbf{r}, t) + \mathbf{P}_R(\mathbf{r}, t)$$
$$= \epsilon_0 \int_{-\infty}^{\infty} \chi_L(t - t')\mathbf{E}(\mathbf{r}, t')\mathrm{d}t' + \epsilon_0 \mathbf{E}(\mathbf{r}, t)$$
$$\times \left[\int_{-\infty}^{\infty} R_N(t - t')F_N(t')\mathrm{d}t' + \chi_K \mathbf{E}(\mathbf{r}, t) \cdot \mathbf{E}(\mathbf{r}, t) + \int_{-\infty}^{\infty} \chi_R(t - t') \times \mathbf{E}(\mathbf{r}, t') \cdot \mathbf{E}(\mathbf{r}, t')\mathrm{d}t' \right]. \quad (1)$$

where $\mathbf{E}(\mathbf{r}, t)$ is the electric field, ϵ_0 is the permittivity of free space, $\chi_L(t)$ is the linear susceptibility, χ_K is the Kerr susceptibility, $\chi_R(t)$ is a third-order time-dependent nonlinear susceptibility that accounts for Raman scattering, $F_N(t)$ is a Langevin noise source representing the driving force that leads to random vibrations of silica molecules, and $R_N(t)$ is the response function that converts $F_N(t)$ into a susceptibility through

$$\chi_N(t) = \int_{-\infty}^{\infty} R_N(t - t')F_N(t')\mathrm{d}t', \quad (2)$$

where $\chi_N(t)$ is a noise susceptibility.

In our previous study two coupled-wave equations were derived by use of the Kerr and Raman nonlinear polarizations.[4] However, the expression for the Raman polarization was limited in accuracy, because the spectrum of the input pump pulse was assumed to be narrow compared with the Raman-gain spectrum. Such an approximation limits the validity to minimum input pump pulse widths of ~1 ps. In what follows, the effect of removing this assumption on the Raman portion of the polarization is discussed. The derivation for the Kerr and noise polarizations remain the same as in Ref. 4.

The electric field and the Raman polarization can be written as the sum of the pump and the Stokes waves and are given, respectively, by

$$\mathbf{E}(\mathbf{r}, t) = \tfrac{1}{2}\hat{x}[E_p(\mathbf{r}, t)\exp(-i\omega_p t) + E_s(\mathbf{r}, t) \times \exp(-i\omega_s t) + \text{c.c.}], \quad (3)$$

$$\mathbf{P}_R(\mathbf{r}, t) = \tfrac{1}{2}\hat{x}[P_{Rp}(\mathbf{r}, t)\exp(-i\omega_p t) + P_{Rs}(\mathbf{r}, t) \times \exp(-i\omega_s t) + \text{c.c.}]. \quad (4)$$

Here $\hat{x}$ is the polarization unit vector; ω_j is the carrier frequency, with the subscript j ($=p$ or s) representing the pump or the Stokes pulse respectively; $E_j(\mathbf{r}, t)$ is the envelope of the electric field; and $P_{Rj}(\mathbf{r}, t)$ is the envelope of the Raman polarization field. Both envelopes are slowly varying compared with the time scale of $1/\omega_j$. A similar expression can be written for the noise force that leads to random molecular vibrations:

$$F_N(z, t) = \tfrac{1}{2}\hat{x}[f_N(z, t)\exp(-i\Omega_R t) + \text{c.c.}], \quad (5)$$

where $f_N(z, t)$ is the slowly varying envelope of the random force and $\Omega_R = \omega_p - \omega_s$ is the vibrational frequency of the molecule and is assumed to be at the peak of the Raman-gain curve. Equations (3)–(5) assume that both the pump and the signal pulses maintain their same states of linear polarization along the x axis. The slowly varying envelope approximation is equivalent to assuming that the pulse spectral width $\Delta\omega_j \ll \omega_j$, a condition that holds true for pulses of widths greater than 10 fs in the visible and the near-infrared regions.

The calculation of the Raman polarization [see Eq. (1)] requires evaluation of the dot product $\mathbf{E} \cdot \mathbf{E}$. Using Eq. (3), we can write this product as

$$\mathbf{E} \cdot \mathbf{E} = \tfrac{1}{2}|E_p|^2 + \tfrac{1}{2}|E_s|^2 + \tfrac{1}{2}E_p E_s^* \times \exp[-i(\omega_p - \omega_s)t] + \tfrac{1}{2}E_p^* E_s \times \exp[i(\omega_p - \omega_s)t] + \tfrac{1}{2}E_p E_s \times \exp[-i(\omega_p + \omega_s)t] + \tfrac{1}{2}E_p^* E_s^* \times \exp[i(\omega_p + \omega_s)t] + \tfrac{1}{4}E_p^2 \exp(-i2\omega_p t) + \tfrac{1}{4}E_p^{*2} \exp(i2\omega_p t) + \tfrac{1}{4}E_s^2 \exp(-i2\omega_s t) + \tfrac{1}{4}E_s^{*2} \exp(i2\omega_s t). \quad (6)$$

Equation (6) is substituted into the Raman-polarization portion given in Eq. (1). All terms except the first four can be dropped, because they require a phase-matching condition. The remaining four terms lead to the following expression for the Raman polarization:

$$P_{Rj}(\mathbf{r}, t) = 1/4\epsilon_0 E_j(t) \int_{-\infty}^{\infty} \chi_R(t - t')[|E_j(t')|^2 + |E_k(t')|^2]\mathrm{d}t' + 1/2\epsilon_0 E_k(t) \times \int_{-\infty}^{\infty} \chi_R(t - t')E_j(t')E_k^*(t') \times \exp[-i(\omega_j - \omega_k)(t' - t)]\mathrm{d}t', \quad (7)$$

where for notational convenience we do not show the $\mathbf{r}$ dependence of the electric field.

To incorporate Eq. (7) into coupled amplitude equations for the pump and the Stokes wave, the starting point is Maxwell's wave equation

$$\nabla^2 \mathbf{E} - \frac{1}{c^2}\frac{\partial^2 \mathbf{E}}{\partial t^2} = \mu_0 \frac{\partial^2 \mathbf{P}}{\partial t^2}, \quad (8)$$

where c is the velocity of light in vacuum and μ_0 is the vacuum permeability. The distribution of the electric field perpendicular to the direction of propagation, $T_j(x, y)$, can be separated out from the amplitude envelope $A_j(z, t)$ of the pump or Stokes pulse, assuming that nonlinear effects do not significantly alter the fundamental fiber-mode distribution $T_j(x, y)$.[1] The electric field is then written as

$$E_j(\mathbf{r}, t) = T_j(x, y)A_j(z, t)\exp(i\beta_{0j}z) \qquad (j = p, s), \quad (9)$$

where β_{0j} is the wave number corresponding to the frequency ω_j. In general $T_p(x, y)$ and $T_s(x, y)$ are different. However, this difference is small enough that the two can be approximated by the same distribution, $T(x, y)$.

One can derive the coupled equations more easily by working in the frequency domain. Using the Fourier transform of Eq. (8), we can calculate the terms in the re-

sulting equation as follows. We find the electric field by substituting Eq. (9) into Eq. (3) and taking the Fourier transform of this result. We find the polarization by taking the Fourier transform of Eq. (1) with $P_R(\mathbf{r}, t)$ given by Eq. (7) and using the previously calculated value of the electric field. By following the method outlined in Ref. 4, which assumes that the nonlinear and noise contributions to $\mathbf{P}_{NL}(\mathbf{r}, t)$ are a small perturbation to the refractive index, we can obtain the following coupled equations for the pump and the Stokes waves:[4,10]

$$\begin{aligned}\frac{\partial u_p}{\partial z} + \frac{1}{v_{gp}}\frac{\partial u_p}{\partial t} + i\frac{\beta_{2p}}{2}\frac{\partial^2 u_p}{\partial t^2} - \frac{\beta_{3p}}{6}\frac{\partial^3 u_p}{\partial t^3} + \frac{\alpha_p}{2}u_p \\ = i\gamma_p(1-f_R)u_p(|u_p|^2 + 2|u_s|^2) + i\gamma_p f_R u_p \\ \times \int_{-\infty}^{\infty} h_r(t-t')[|u_p(t')|^2 \\ + |u_s(t')|^2]\mathrm{d}t' + i\gamma_p f_R u_s \\ \times \int_{-\infty}^{\infty} h_r(t-t')u_p(t')u_s{}^*(t')\exp[i\Omega_R(t-t')]\mathrm{d}t' \\ + iu_s\int_{-\infty}^{\infty} h_p(t-t')f_N(z,t')\exp[i\Omega_R(t-t')]\mathrm{d}t'\end{aligned} \tag{10}$$

$$\begin{aligned}\frac{\partial u_s}{\partial z} + \frac{1}{v_{gs}}\frac{\partial u_s}{\partial t} + i\frac{\beta_{2s}}{2}\frac{\partial^2 u_s}{\partial t^2} - \frac{\beta_{3s}}{6}\frac{\partial^3 u_s}{\partial t^3} + \frac{\alpha_s}{2}u_s \\ = i\gamma_s(1-f_R)u_s(|u_s|^2 + 2|u_p|^2) + i\gamma_s f_R u_s \\ \times \int_{-\infty}^{\infty} h_r(t-t')[|u_s(t')|^2 \\ + |u_p(t')|^2]\mathrm{d}t' + i\gamma_s f_R u_p \\ \times \int_{-\infty}^{\infty} h_r(t-t')u_s(t')u_p{}^*(t') \\ \times \exp[-i\Omega_R(t-t')]\mathrm{d}t' \\ + iu_p\int_{-\infty}^{\infty} h_s(t-t')f_N^*(z,t') \\ \times \exp[-i\Omega_R(t-t')]\mathrm{d}t'.\end{aligned} \tag{11}$$

The field amplitude has been normalized such that

$$u_j = \kappa A_j\left[\int_{-\infty}^{\infty} T^2(x,y)\mathrm{d}x\mathrm{d}y\right]^{1/2},$$

$$\kappa^2 = {}^1\!/_2 n_j(\epsilon_0/\mu_0)^{1/2}. \tag{12}$$

κ was introduced to normalize u_j such that $|u_j|^2$ represents power and n_j is the linear index of the fiber. We have combined the Kerr and Raman susceptibilities into the nonlinear coefficient γ_j by using the definitions

$$\gamma_j = \frac{\omega_j n_2}{cA_{\mathrm{eff}}\,\kappa^2}, \quad n_2 = \frac{3}{8n_j}\chi_K\left(1 + \frac{2\chi_0}{3\chi_K}\right),$$

$$\chi_R(t) = \chi_0 h_r(t), \quad A_{\mathrm{eff}} = \frac{\left(\int_{-\infty}^{\infty}\int_{-\infty}^{\infty} T^2\mathrm{d}x\mathrm{d}y\right)^2}{\int_{-\infty}^{\infty}\int_{-\infty}^{\infty} T^4\mathrm{d}x\mathrm{d}y}, \tag{13}$$

where n_2 is the nonlinear refractive index, χ_0 is the peak value of $\chi_R(t)$, and A_{eff} is the effective core area of the fiber. f_R is the fraction of the nonlinearity that arises because of molecular vibrations and is given as

$$f_R = \left(1 + \frac{3\chi_K}{2\chi_0}\right)^{-1}. \tag{14}$$

Finally, $h_p(t)$ and $h_s(t)$ are the response functions for the noise term, calculated as

$$h_j(t) = \frac{\omega_j R_N(t)}{4cn_j} \qquad (j = p, s). \tag{15}$$

Various terms in Eqs. (10) and (11) have the following physical interpretation: The first term describes how the pulse envelope changes with distance. The next three terms represent the effects of the group velocity, the group-velocity dispersion, and the third-order dispersion. The last term on the left-hand side of each equation is for the fiber loss. The first two terms on the right-hand side of each equation include the Kerr-induced (electronic) contribution to self-phase modulation and cross-phase modulation (XPM), respectively. The next two terms represent the molecular contribution to self-phase modulation and cross-phase modulation, respectively, as well as describing the interpulse SFS and the intrapulse CFS. The next term on the right is responsible for Raman amplification, and the final term describes spontaneously scattered noise in the fiber. The role of the Raman terms is further explained in Section 4.

Equations (10) and (11) are valid for pulse widths up to the limit of the slowly varying envelope approximation (~10 fs). However, for pulse widths greater than 1 ps certain simplifying assumptions can be made. Before considering the role of the SFS and the CFS on SRS process, we examine in Section 3 the approximations that can made be for picosecond pump pulses.

3. PICOSECOND REGIME

To understand the approximations that can be made for picosecond pump pulses, consider the two terms proportional to f_R on the right-hand sides of Eqs. (10) and (11):

$$\begin{aligned}\Re_j(t) = i\gamma_j f_R u_j\int_{-\infty}^{\infty} h_r(t-t')[|u_j(t')|^2 + |u_k(t')|^2]\mathrm{d}t' \\ + i\gamma_j f_R u_k\int_{-\infty}^{\infty} h_r(t-t')u_j(t')u_k{}^*(t') \\ \times \exp[-i\Omega_R(t-t')]\mathrm{d}t',\end{aligned} \tag{16}$$

where it should be noted that the sign of the exponent changes when $j = p$. For relatively broad pulse widths (>1 ps), u_j and u_k can be treated as constants compared with the time scale under which $h_r(t)$ is varying. Equation (16) can then be written as

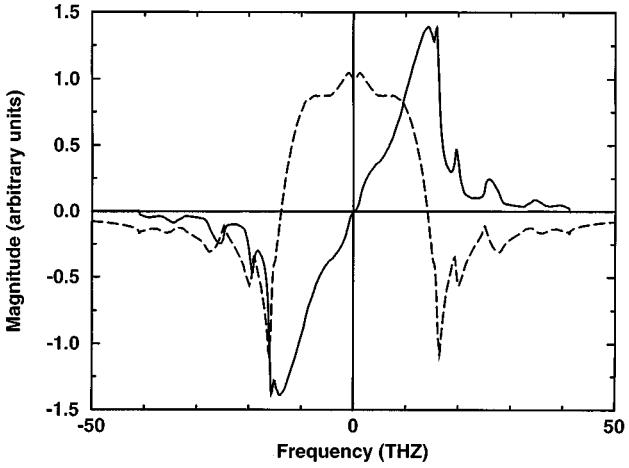

Fig. 1. Imaginary (solid curve) and real (dashed curve) parts of the Raman response function. The imaginary portion $h_r''(\omega)$ is proportional to Raman gain, and the real part $h_r'(\omega)$ is proportional to Raman-induced index changes.

$$\Re_j(t) = i\gamma_j f_R u_j(t)[|u_j(t)|^2 + |u_k(t)|^2]\int_{-\infty}^{\infty} h_r(t-t')\mathrm{d}t' + i\gamma_j f_R u_j(t)|u_k(t)|^2\int_{-\infty}^{\infty} h_r(t-t') \times \exp[-i\Omega_R(t-t')]\mathrm{d}t'. \quad (17)$$

The normalization of the response function in Eq. (13) means that the first integral in Eq. (17) is equal to 1. The second integral is equal to the Fourier transform, $\tilde{h}_r(\omega)$, of the Raman response function evaluated at frequency $\omega = \Omega_R$. The real $[\tilde{h}_r'(\omega)]$ and the imaginary $[\tilde{h}_r''(\omega)]$ parts of $\tilde{h}_r(\omega)$ are plotted in Fig. 1. $\tilde{h}_r'(\omega)$ is responsible for Raman-induced index changes, whereas $\tilde{h}_r''(\omega)$ is responsible for the Raman gain. The Raman-gain spectrum is quite wide (~10 THz); therefore pulse spectral widths below ~0.5 THz can be considered small enough that the spectra of such pulses are nearly delta functions. This spectral width corresponds to temporal pulse widths of ~1 ps. Equation (17) can now be written as

$$\Re(t) = i\gamma_j f_R u_j(t)[|u_j(t)|^2 + |u_k(t)|^2] - \gamma_j \tilde{f}_R h_r''(-\Omega_R)u_j(t)|u_k(t)|^2, \quad (18)$$

where $\tilde{h}_r(-\Omega_R) = i\tilde{h}_r''(-\Omega_R)$ at the peak of the Raman-gain curve, as can be seen from Fig. 1, has been used. Finally, the Raman-gain coefficient g_j can be defined as

$$g_j = 2 f_R \gamma_j |\tilde{h}_r''(\Omega_R)|. \quad (19)$$

Using Eqs. (18) and (19), we can write coupled amplitude equations for the picosecond regime as

$$\frac{\partial u_p}{\partial z} + \frac{1}{v_{gp}}\frac{\partial u_p}{\partial t} + i\frac{\beta_{2p}}{2}\frac{\partial^2 u_p}{\partial t^2} + \frac{\alpha_p}{2}u_p = i\gamma_p u_p[|u_p|^2 + (2-f_R)|u_s|^2] - \frac{g_p}{2}u_p|u_s|^2, \quad (20)$$

$$\frac{\partial u_s}{\partial z} + \frac{1}{v_{gs}}\frac{\partial u_s}{\partial t} + i\frac{\beta_{2s}}{2}\frac{\partial^2 u_s}{\partial t^2} + \frac{\alpha_s}{2}u_s = i\gamma_s u_s[|u_s|^2 + (2-f_R)|u_p|^2] + \frac{g_s}{2}u_s|u_p|^2, \quad (21)$$

where the third-order dispersion is neglected for picosecond pulse widths and it is assumed that both the pump and the Stokes pulses are incident at the fiber so the noise in the fiber is negligible compared with the input power of these pulses. The factor of $2 - f_R$ as opposed to 2 for the XPM term was explained in Ref. 11. It is worthwhile to note that the ratio of Raman gain to the nonlinear parameter, $q = g_p/\gamma_p$,[5,6] is generally approximated by 0.5. This ratio can be used as a check of Eqs. (20) and (21) by use of the new variables presented in this paper. Such a calculation yields

$$q = \frac{g_p}{\gamma_p} = 2 f_R \tilde{h}_r'(\Omega_R) = 0.50, \quad (22)$$

where a widely accepted value of $f_R = 0.18$ (Ref. 9) and a value of $\tilde{h}_r''(\omega_R) = 1.38$ from Fig. 1 have been used. The calculated value of q agrees with the accepted value of 0.5.

The coupled amplitude equations are best suited for the case of Raman amplification in which both the pump and the Stokes pulses are incident at the fiber input end. However, when there is no input Stokes pulse, and a Stokes pulse is formed through Raman generation, the assumption that the Stokes pulse spectrum is narrow compared with the Raman-gain curve is not initially valid. The reason is that the Stokes pulse builds up from noise whose spectral width can be considered as broad as the Raman-gain spectrum. This was the case studied in Ref. 4. By following the procedure outlined above and in Ref. 4 we can write the coupled equations for Raman generation as

$$\frac{\partial u_p}{\partial z} + \frac{1}{v_{gp}}\frac{\partial u_p}{\partial t} + i\frac{\beta_{2p}}{2}\frac{\partial^2 u_p}{\partial t^2} = i\gamma_p u_p[|u_p|^2 + (2-f_R)|u_s|^2] + i1/2u_p u_s\int_{-\infty}^{\infty} g_p(t-t') \times u_s^*(t')\exp[i\Omega_R(t-t')]\mathrm{d}t' + iu_s\int_{-\infty}^{\infty} h_p \times (t-t')f_N(z,t')\exp[i\Omega_R(t-t')]\mathrm{d}t', \quad (23)$$

$$\frac{\partial u_s}{\partial z} + \frac{1}{v_{gs}}\frac{\partial u_s}{\partial t} + i\frac{\beta_{2s}}{2}\frac{\partial^2 u_s}{\partial t^2} = i\gamma_s u_s[|u_s|^2 + (2-f_R)|u_p|^2] + i1/2|u_p|^2 \times \int_{-\infty}^{\infty} g_s(t-t')u_s(t')\exp[-i\Omega_R(t-t')]\mathrm{d}t' + iu_p \times \int_{-\infty}^{\infty} h_s(t-t')f_N^*(z,t')\exp[-i\Omega_R(t-t')]\mathrm{d}t'. \quad (24)$$

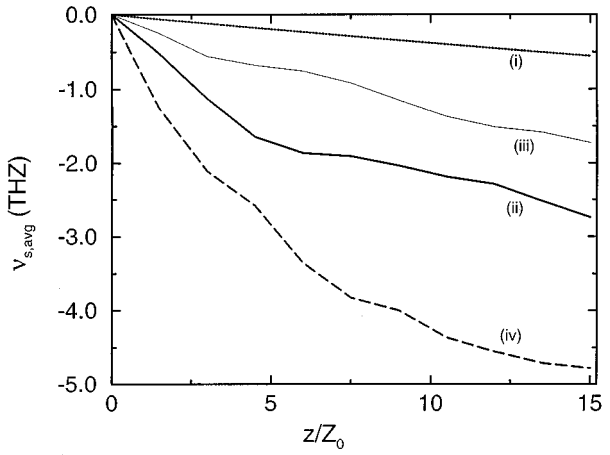

Fig. 2. Change in the mean frequency as a function of distance for (i) a fundamental soliton, (ii) two copropagating fundamental solitons with no interpulse SRS, (iii) two copropagating fundamental solitons with no interpulse SRS and no XPM, and (iv) two copropagating fundamental solitons. Parameters are $t_p = t_s = 100$ fs, $\beta_{2p} = -5$ ps^2 km^{-1}, $\beta_{2s} = -5.35$ ps^2 km^{-1}, $\gamma_p = 3.50$ km^{-1} W^{-1}, $\gamma_s = 3.27$ km^{-1} W^{-1}, $P_{0p} = 143$ W, and $P_{0s} = 164$ W.

4. SUBPICOSECOND REGIME

For pump pulse widths of $\lesssim 1$ ps the assumption that the spectrum of the pump and the Stokes pulses is narrow compared with the Raman-gain spectrum is no longer valid. The full Raman term given in Eq. (16) must then be used. We can best explain the role of each term in the frequency domain by calculating the Fourier transform of Eq. (16):

$$\begin{aligned}\tilde{\Re}_j(\omega) = {} & i\gamma_j f_R \int_{-\infty}^{\infty}\int_{-\infty}^{\infty} \tilde{h}_r(\omega_1)\tilde{u}_j(\omega - \omega_1) \\ & \times \tilde{u}_j(\omega_1 - \omega_2)\tilde{u}_j{}^*(-\omega_2)\mathrm{d}\omega_2\mathrm{d}\omega_1 \\ & + i\gamma_j f_R \int_{-\infty}^{\infty}\int_{-\infty}^{\infty} \tilde{h}_r(\omega_1)\tilde{u}_j(\omega - \omega_1) \\ & \times \tilde{u}_k(\omega_1 - \omega_2)\tilde{u}_k{}^*(-\omega_2)\mathrm{d}\omega_2\mathrm{d}\omega_1 \\ & + i\gamma_j f_R \int_{-\infty}^{\infty}\int_{-\infty}^{\infty} \tilde{h}_r(\omega_1 - \Omega_R)\tilde{u}_j(\omega_1 - \omega_2) \\ & \times \tilde{u}_k(\omega - \omega_1)\tilde{u}_k^*(-\omega_2)\mathrm{d}\omega_2\mathrm{d}\omega_1, \end{aligned} \tag{25}$$

where again the sign of Ω_R changes for $j = p$. The major contribution to the first two terms in Eq. (25) comes when $\omega_1 = 0$ and $\omega = -\omega_2 = \omega_j$ for the first term and $\omega_1 = 0$, $\omega = \omega_j$, and $\omega_2 = -\omega_k$ for the second term [for these values $\tilde{h}_r(\omega)$ has only a phase contribution]. For all other combinations the integrand becomes relatively small. For the nonzero combination of ω, ω_1, and ω_2, as the pulse spectrum broadens the contribution from the imaginary portion of $\tilde{h}_r(0)$ increases. Figure 1 shows that half of the spectral components of the pump pulse see $\tilde{h}_r{}''$ of one sign and the other half see $\tilde{h}_r{}''$ with the opposite sign. The result is that there is a transfer of energy within the pulse from the high-frequency components to the low-frequency components and the mean frequency of the pulse is constantly decreasing. For the first term of Eq. (7) this spectral shift results in a SFS, whereas for the second term the spectral shift is induced because of the presence of another copropagating pulse, a (Raman-induced) CFS.[8] The third term in Eq. (25) is responsible for Raman amplification of the Stokes pulse. Equations (10) and (11) are valid up to the limit of the slowly varying envelope approximation ($\Delta\omega_j \ll \omega_j$) or for pump pulse as short as 10 fs. In the following subsections the effect of the CFS on copropagating solitons and the effect of the SFS on Raman generation are studied.

A. Cross-Frequency Shift

A numerical code was written based on the fast-Fourier-transform split-step method[1] to simulate evolution of the pump and the Stokes pulses as described by Eqs. (10) and (11). The convolution integrals were evaluated by multiplication of the Fourier transform of the appropriate variables, followed by an inverse Fourier transform of the result. The noise term is simulated by the generation of random numbers with a Gaussian distribution of zero mean and unit variance. The integrals in Eqs. (10) and (11) were included in the nonlinear operator used in the fast-Fourier-transform split-step method.[1] We quantified the effects of the SFS and the CFS by calculating the mean frequency $\nu_{j,\mathrm{avg}}$ of the pulse spectrum. This quantity is defined as

$$\nu_{j,\mathrm{avg}}(z) = \frac{\int \nu|\tilde{u}_j(z,\nu)|^2\mathrm{d}\nu}{\int |\tilde{u}_j(z,\nu)|^2\mathrm{d}\nu} \qquad (j = p, s), \tag{26}$$

where $\tilde{u}_j(z, v)$ is the Fourier transform of $u_j(z, t)$.

Figure 2 is a plot of the mean frequency versus distance for the Stokes pulse, copropagating with a pump pulse. Both pulses are initially fundamental solitons with a profile $u_j(0, t) = \sqrt{P_{0j}}\,\mathrm{sech}(t/t_j)$, such that N, the order of the soliton, is 1, where N is defined as

$$N^2 = \frac{\gamma_p P_{0p} {t_p}^2}{|\beta_{2p}|} = \frac{\gamma_s P_{0s} {t_s}^2}{|\beta_{2s}|}. \tag{27}$$

The parameters used in the simulations are $t_p = t_s = 100$ fs, $\beta_{2p} = -5$ ps^2/km, $\beta_{2s} = -5.35$ ps^2/km, $\gamma_p = 3.50$ (km W)$^{-1}$, $\gamma_s = 3.27$ (km W)$^{-1}$, $P_{0p} = 143$ W, and $P_{0s} = 164$ W. The effect of pulse walk-off is neglected, and Raman amplification is negligible because of the small frequency difference between the pulses. This corresponds to a situation such as a wavelength-division-multiplexing scheme in which the wavelength difference between the pump and the Stokes pulses can be 1–2 nm. The length of fiber used is expressed as a function of the soliton period Z_0, defined as

$$Z_0 = \frac{\pi}{2}\frac{t_p^2}{|\beta_{2p}|}. \tag{28}$$

Curve (i) of Fig. 2 is for the case of a Stokes pulse propagating by itself, curve (ii) shows the effect on the Stokes pulse of adding a copropagating pump pulse but neglecting the CFS, curve (iii) is the same as curve (ii) with the XPM terms in Eqs. (10) and (11) set equal to 0, and finally curve (iv) is the same as curve (ii) with the CFS included. Curve (i) is shown for reference and represents the well-

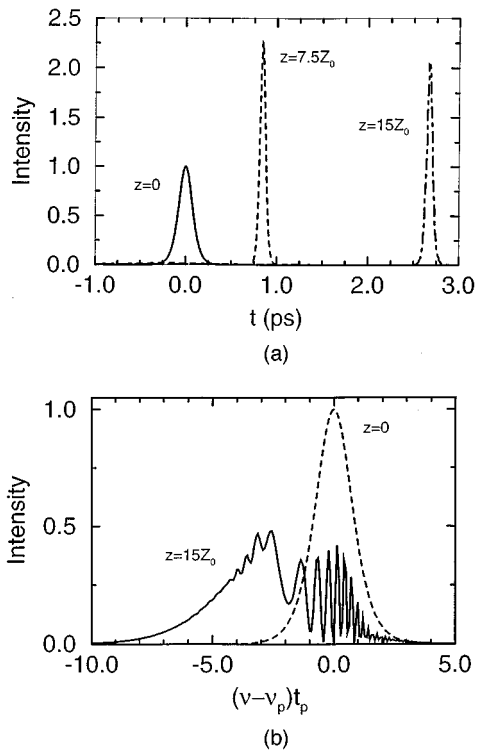

Fig. 3. (a) Shapes and (b) spectra of the Stokes pulse, showing the effect of intrapulse stimulated Raman scattering when the Stokes pulse copropagates with a pump pulse. Input powers for both pulses correspond to a fundamental soliton.

known soliton SFS. This result was obtained by simulations in which $u_p(0, t) = 0$ and the spontaneous Raman noise is neglected. The effect of noise in the fiber is studied in Subsection 4.B in the context of a Raman generator.

Curve (ii) shows that the presence of a pump pulse, even when one does not consider interpulse SRS, leads to a significant increase in the frequency shift of the Stokes pulse, from -0.55 to -2.7 THz at $z/Z_0 = 15$. The reason for this becomes clear from Fig. 3. Figure 3(a) is a plot of the Stokes pulse for several lengths of fiber when pump and the Stokes pulses propagate simultaneously. It shows that the Stokes pulse has shed some of its energy and a narrower pulse has evolved. The SFS increases inversely with the fourth power of the pulse width[6]; therefore the narrower pulse experiences an increased frequency shift. This can be seen in the plot of the Stokes pulse spectrum at $15Z_0$ in Fig. 3(b). The portion of the spectrum that is shifted out to the red side of the spectrum represents the narrow spike that has split off. There is a simple intuitive explanation for this behavior. It is well known that during the propagation of higher-order solitons the presence of intrapulse SRS causes the pulse to shed some of its energy into a dispersive wave and evolve into a shorter pulse. This shorter pulse then downshifts in frequency in a manner similar to that observed in Fig. 3(a).[12] The situation here is analogous. In the presence of a second pulse, the nonlinear induced chirp on the soliton comes from both SPM and XPM. This increased nonlinearity is equivalent to having an increased input power or a higher-order soliton; hence the same splitting of the pulse spectrum occurs that would occur for higher-order solitons.

To verify the explanation that the copropagating solitons behave as higher-order solitons, we obtained results for the pump and the Stokes pulses by including the SFS and the CFS but with the XPM term artificially set to zero. Curve (iii) of Fig. 2 shows that the frequency shift experienced by the pulse is larger than that which occurs for the case of a single soliton propagating in the fiber but not so large as that obtained when XPM is included [curve (ii)]. The increase is due to the additional frequency shift introduced by the CFS effect. As expected, plots of the pulse shape and spectra show no pulse splitting taking place.

Finally, the contribution to the process of the CFS can be studied by comparison of curves (ii) and (iv) in Fig. 2. The CFS increases the frequency shift seen compared with that seen when the pulse is traveling alone. The frequency shift changes from -2.2 to -4.7 THz after $15Z_0$. Equations (10) and (11) predict this increase because the additional contribution provided by interpulse SRS is of the same order of magnitude as it is for intrapulse SRS. This increase is more than doubled because the solitons evolve into narrower solitons with higher peak powers. Plots of the pulse shape and spectrum that correspond to curve (iv) show the same qualitative behavior as those seen in Fig. 3.

B. Effect of the Self-Frequency Shift on Raman Generation

In Subsection 4.A it was seen that the SFS leads to a frequency downshift in the spectrum of a fundamental soliton. This affects Raman generation as follows. Because of the SFS any Stokes pulse generated will have less energy than it would have in the absence of intrapulse SRS. This is because the pump pulse's frequency is downshifting, and therefore the frequency of the spontaneous Raman noise's being amplified is changing. If the spectral downshift occurs over lengths of fiber that are too short to permit significant amplification of noise at a given frequency, then a Stokes pulse will not be generated.

To explore the Raman generation process during a SRS-induced SFS, we carried out numerical simulations with femtosecond pump pulses. To facilitate the discussion, two length scales are introduced, the dispersion length L_D and the walk-off length L_w. These lengths are defined, respectively, as[1]

$$L_D = \frac{{t_p}^2}{|\beta_{2p}|}, \qquad L_W = \frac{t_p}{|d|}, \tag{29}$$

where d is a walk-off parameter defined as the difference between the inverse of the group velocities of the pump and the Stokes pulses, respectively.[1] L_D and L_w describe, respectively, the length scales over which group-velocity dispersion and walk-off become important. During Raman generation walk-off effects are not negligible because the frequency difference between the pump pulse and the Stokes pulse generated is $\sim$13.2 THz, the frequency at which the maximum Raman gain occurs. One can use the walk-off length to calculate the threshold power P_{th} by using the criterion[1]

$$g_p P_{\text{th}} L_w \geq 16. \tag{30}$$

If first-order solitons are used, the length of fiber necessary for Raman generation to be seen would be much larger than L_w. For example, the peak power for a fundamental soliton with $t_p = 100$ fs, $\gamma_p = 3.5$ $(\text{W km})^{-1}$, and $\beta_2 = -5$ ps^2/km is 143 W. Using inequality (30) with $g_p = 1.75$ $(\text{W km})^{-1}$, we calculate that $L_w \geq 64$ m. The pulses would have to separate by less than 100 fs in the 64 m of fiber or have a walk-off of less than 1.56 fs/m, a number so small that this is the equivalent to saying that there should be no walk-off between the pulses. Hence higher-order solitons are used to reduce the fiber length necessary to achieve Raman generation. For the dispersion-shifted fiber under consideration, pulses shorter than ~1 ps satisfy the criterion that $L_D < L_w$. Thus walk-off can be neglected for fiber lengths less than L_D. To determine the input pump power necessary, one can use inequality (30) in conjunction with Eq. (27). From Eq. (22) the relationship $g_p = \gamma_p/2$ is substituted into inequality (30) along with $L_w = L_D$. The resulting threshold power is used as the input power P_0 in Eq. (27) to give $N^2 = 32$. The value of N is raised to 6, the nearest integer, and the input peak power is calculated for an $N = 6$ soliton with $\beta_{2p} = -5$ ps^2/km and $\gamma_p = 3.5$ $(\text{W km})^{-1}$. The results of these calculations are shown in Table 1.

Figure 4(a) shows the results that we obtained by propagating a 1-ps pump pulse with the parameters given in Table 1 and with $\gamma_s = 3.27$ $(\text{km W})^{-1}$, $g_s = 1.63$ $(\text{km W})^{-1}$, and $\beta_{2s} = -5$ ps^2/km. The results show that after a distance of Z_0 two Stokes pulses have formed. This occurs because initially a splitting of the pump pulse owing to intrapulse SRS occurs. The first pump pulse that splits away from the main pulse excites a Stokes pulse, which eventually depletes the copropagating portion of the pump pulse. Meanwhile, a second pulse, which has split off from the main pump pulse, also begins to excite a Stokes pulse. This pulse has a smaller peak power because the second pump pulse has not been completely depleted. A plot of the Stokes spectrum in Fig. 4(b) shows that the Stokes pulse spectrum is itself undergoing a frequency downshift. Simulations of longer fiber lengths show that the first Stokes pulse seen in Fig. 4 maintains its intensity and width. Examination of the energy lost by the pump pulse reveals that the pump pulse loses 45% of its energy to the first Stokes pulse, and at L_D it has lost an additional 14% to the second Stokes pulse.

The results of propagating a 100-fs, $N = 6$ soliton over L_D show the characteristic splitting of the pump pulse that is due to intrapulse SRS; however, unlike in the previous results, there is no Stokes pulse generated from noise. The frequency of the pump pulse has shifted by −29.7 THz after one dispersion length, or more than the 13.2-THz Stokes shift. Although there is some energy at the Stokes frequency, most of it belongs to the pump pulse. Simulations with the interpulse and intrapulse SRS terms turned off show that over the same distance a

Table 1. Pulse Width, Dispersion Length, and Input Pump Power for $N = 6$ Soliton with $g_p = 1.75$ $(\text{km W})^{-1}$ and $\beta_{2p} = -5$ ps^2/km

t_p	L_D (m)	P_0 (W)
1 ps	200	51.4
500 fs	50	205.7
100 fs	2	5140

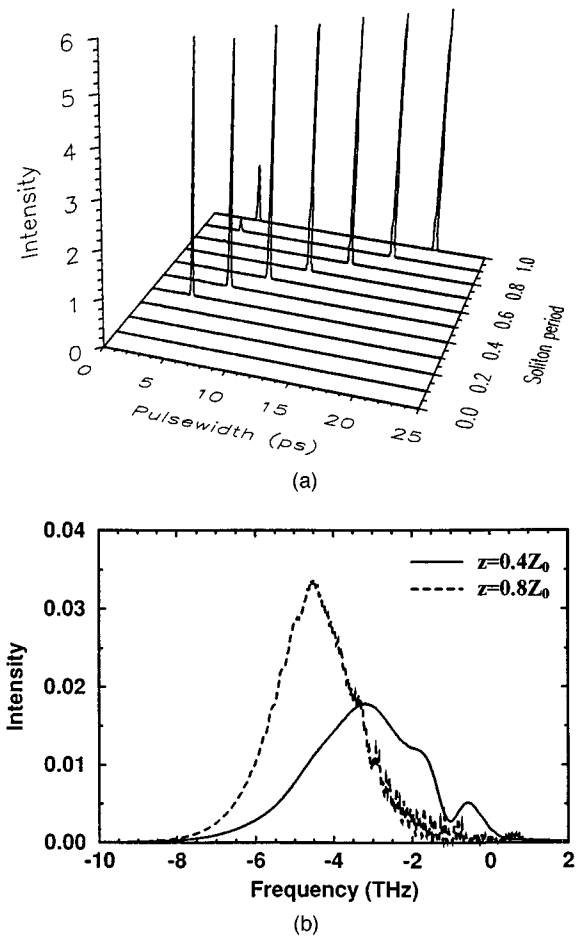

Fig. 4. (a) Shapes and (b) spectra showing the growth of the Stokes pulse from noise during the propagation of a sixth-order soliton with parameters $t_p = t_s = 1$ ps, $\beta_{2p} = -5$ $\text{ps}^2\,\text{km}^{-1}$, $\beta_{2s} = -5.35$ $\text{ps}^2\,\text{km}^{-1}$, $\gamma_p = 3.50$ $\text{km}^{-1}\,\text{W}^{-1}$, $\gamma_s = 3.27$ $\text{km}^{-1}\,\text{W}^{-1}$, $g_p = 1.75$ $\text{km}^{-1}\,\text{W}^{-1}$, and $g_s = 1.63$ $\text{km}^{-1}\,\text{W}^{-1}$.

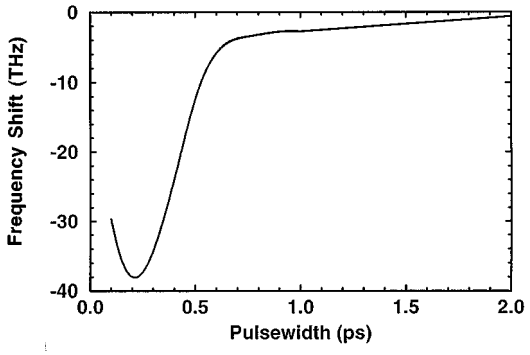

Fig. 5. Frequency shift plotted as a function of the pulse width experienced by a sixth-order soliton over one dispersion length.

Stokes pulse with a peak intensity of 310 W develops if SFS does not occur. Clearly SFS is detrimental to Raman generation for femtosecond pump pulses.

To set a limit on the minimum width of the pump pulse for which Raman generation can occur, an expression for the frequency shift experienced by the pulse would be useful. Such an expression was derived in Ref. 6 for a fundamental soliton and in Ref. 8 for copropagating pulses. However, these results assumed that the pulse shape was not changing during propagation, which is clearly not the case here. To find an expression for the frequency shifts described here one would need an analytical expression for the variation of pulse shape with propagation. To the best of our knowledge, no such analytical solution exists. Therefore, to quantify the frequency shift experienced by an $N = 6$ soliton, we conducted the simulations for various pump pulse widths with the noise term neglected. The results, showing a frequency shift after one dispersion length as a function of pulse width, are shown in Fig. 5. It should be noted that the decrease in frequency shift after 200 fs corresponds to a decrease in $h_r(t)$ as illustrated in Fig. 1 of Ref. 6.

5. CONCLUSIONS

In this paper coupled nonlinear Schrödinger equations that account for Raman amplification, generation, and the SRS-induced SFS and CFS in a unified manner are presented. These equations are valid as long as the slowly varying envelope approximation is valid (pulse widths as short as 10 fs). For picosecond pulses these equations reduce to the standard equations.

The coupled nonlinear Schrödinger equations were used to study the effect of the CFS on copropagating solitons. The results show that when a splitting of the solitons occurs that is similar to that which occurs when a single higher-order soliton travels under the influence of the soliton SFS, the frequency shift of the pulse increases as the result of the CFS. It was also shown that the SFS reduces the amount of energy transferred to the Stokes pulse during Raman generation. As the pulse width is reduced below 1 ps, the pulse spectrum downshifts bysuch a large amount that the concept of a distinct Stokes pulse becomes meaningless.

REFERENCES

1. G. P. Agrawal, *Nonlinear Fiber Optics*, 2nd ed. (Academic, San Diego, California, 1995).
2. K. X. Liu and E. Garmire, "Understanding the formation of the SRS Stokes spectrum in fused silica fibers," IEEE J. Quantum Electron. **27**, 1022–1030 (1991).
3. V. A. Aleshkevich, G. D. Kozhoride, and M. V. Shamonin, "Generation of Stokes stimulated Raman scattering pulses from spontaneous noise in fiber lightguides," J. Commun. Technol. Electron. **38**, 104–109 (1993).
4. C. Headley III and G. P. Agrawal, "Noise characteristics of picosecond Stokes pulses generated in optical fibers through stimulated Raman scattering," IEEE J. Quantum Electron. **31**, 2058–2067 (1995).
5. C. Headley III and G. P. Agrawal, "Simultaneous amplification and compression of picosecond optical pulses during Raman amplification in optical fibers," J. Opt. Soc. Am. B **10**, 2383–2389 (1993).
6. J. P. Gordon, "Theory of the soliton self-frequency shift," Opt. Lett. **11**, 662–664 (1986).
7. K. J. Blow and D. Wood, "Theoretical description of transient stimulated Raman scattering in optical fibers," IEEE J. Quantum Electron. **25**, 2665–3673 (1989).
8. S. Kumar, A. Selvarajan, and G. V. Anand, "Influence of Raman scattering on the cross phase modulation in optical fibers," Opt. Commun. **102**, 329–335 (1993).
9. R. H. Stolen, J. P. Gordon, W. J. Tomlinson, and H. A. Haus, "Raman response function of silica-core fibers," J. Opt. Soc. Am. B **6**, 1159–1166 (1989).
10. C. Headley III, "Ultrafast stimulated Raman scattering in optical fibers," Ph.D. dissertation (University of Rochester, Rochester, N.Y., 1995).
11. A. Höök, "Influence of stimulated Raman scattering on cross-phase modulation between waves in optical fibers," Opt. Lett. **17**, 115–117 (1992).
12. G. P. Agrawal, "Effect of intrapulse stimulated Raman scattering on soliton-effect pulse compression in optical fibers," Opt. Lett. **15**, 224–226 (1990).